 Human Molecular Genetics, 2000, Vol. 9, No. 5 769–778

# Germline and somatic loss of function of the mouse *cpk* gene causes biliary ductal pathology that is genetically modulated

**Lisa M. Guay-Woodford[1,2,+], William J. Green[1], J. Russell Lindsey[3] and David R. Beier[4]**

Departments of [1]Medicine, [2]Pediatrics and [3]Comparative Medicine, University of Alabama at Birmingham, Birmingham, AL 35294, USA and [4]Genetics Division, Brigham and Women's Hospital and Harvard Medical School, Boston, MA 02115, USA

Received 23 November 1999; Revised and 14 Accepted January 2000

**The mouse *cpk* mutation is the most extensively characterized murine model of polycystic kidney disease (PKD) and closely resembles human autosomal recessive PKD (ARPKD), with the exception that B6-*cpk*/*cpk* homozygotes do not express the biliary ductal plate malformation (DPM) lesion. However, homozygous mutants from outcrosses to other strains, e.g. DBA/2J (D2), CD-1, BALB/*c* and *Mus mus castaneus* (CAST), express the DPM. The current study was designed: (i) to characterize the *cpk*-associated biliary disease in affected $F_2$ homozygotes from intercrosses with either CAST or D2; and (ii) to evaluate focal biliary cysts identified in heterozygotes from a *D2-cpk* congenic strain. We found that all $F_2$ *cpk*/*cpk* pups expressed both the typical renal cystic disease and the DPM. The DPM severity, assessed using semi-quantitative histopathological analysis, was markedly variable in these $F_2$ progeny. We found no correlation between the severity of the DPM and the renal cystic disease in either $F_2$ cohort. In addition, we identified focal cysts, apparently of biliary origin, in the livers of both aged *D2-+/cpk* and $F_1$ heterozygotes. Genetic analysis demonstrated loss of heterozygosity at the *cpk* interval and supports a loss-of-function model for biliary cysts. We conclude that the *cpk* allele contains an inactivating mutation which disrupts tubulo-epithelial differentiation in the kidney and biliary tract. Expression of the biliary lesion is modulated by genetic background, and the specific biliary phenotype is determined by whether loss of function of the *cpk* gene occurs as a germline or a somatic event.**

## INTRODUCTION

Data from both human and experimental animal models of polycystic kidney disease (PKD) indicate that PKD genes play a fundamentally important role in tubulo-epithelial differentiation of both the kidney and the biliary tract. The identification of these PKD genes and the characterization of the molecular pathways in which they operate should provide important insights into the molecular mechanisms involved in normal epithelial differentiation as well as in PKD pathogenesis.

The biological complexity of these pathogenic pathways is suggested by the wide phenotypic variability in disease phenotypes (reviewed in refs 1–3). The mechanisms underlying this broad phenotypic variability include: (i) mutations in different disease genes; (ii) different mutations within the same disease gene; (iii) random somatic mutations in the wild-type allele, e.g. in autosomal dominant PKD (ADPKD); and (iv) genetic modifiers and/or environmental factors which modulate the expression of specific disease susceptibility genes. Among these various mechanisms, the identification of modifier genes that affect these single gene traits may provide particularly revealing insights into the molecular pathogenesis of PKD.

Such complex genetic interactions can be probed in mouse models far more easily than is possible in human families. Numerous mouse models of PKD have been described in which the mutant phenotypes closely resemble human PKD with regard to morphology, cyst localization and disease progression (4–18). Moreover, genetic background appears to affect the PKD phenotype in these mouse models. Using experimental mouse crosses, these modifying effects can be dissected into discrete genetic factors referred to as quantitative trait loci (QTLs) (19). Recently, QTLs that modulate the renal cystic disease phenotype have been mapped in several mouse PKD models (20–25).

Among the mouse PKD models, the mouse *cpk* mutation has been the most extensively characterized. When expressed on the C57BL/6J (B6) background, the *cpk* gene causes a rapidly progressive renal cystic disease in affected homozygotes that closely resembles human autosomal recessive PKD (ARPKD). Death, presumably due to renal failure, occurs in B6-*cpk/cpk* homozygotes by 3–4 weeks of age. However, unlike ARPKD, the ductal plate malformation (DPM) of the developing biliary tree is not expressed in B6-*cpk*/*cpk* homozygotes (2,4). Yet, when *cpk* is outcrossed to other strains such as DBA/2J (D2), CD-1 and BALB/c, a DPM lesion is expressed in homozygous mutants (5,26,27).

We previously have mapped the *cpk* locus to a <1 cM interval on mouse chromosome 12 (28). We and others (22) have noted that when *cpk* is outcrossed to either the D2 or *Mus mus*

[+]To whom correspondence should be addressed. Tel: +1 205 934 7308; Fax: +1 205 975 5689; Email: lgw@uab.edu

*castaneus* (CAST) strains, the progression of the renal cystic disease in $F_2$ *cpk/cpk* pups is both more accelerated and variable than in B6-*cpk/cpk* pups. Moreover, the DPM is expressed in all $F_2$ mutants. Taken together, these data indicate that genetic modifiers in these experimental crosses modulate the severity of renal cystic disease and unmask a developmental abnormality in biliary differentiation.

The current study was designed: (i) to characterize as a quantitative trait the *cpk*-associated DPM in affected $F_2$ homozygotes from intercrosses with either the CAST or D2 inbred strains; (ii) to determine whether the severity of the renal cystic disease correlated with the severity of the DPM, when both were measured as a quantitative traits; and (iii) to evaluate the focal biliary cysts that we have identified in heterozygotes from a *D2-cpk* congenic strain. We reasoned that these investigations would serve as the first step towards identifying genetic modifiers that modulate the renal and biliary phenotypes in the *cpk* model.

## RESULTS

### Analysis of the $F_2$ cohorts

From the (B6 × CAST) intercross, we examined 22 $F_2$ *cpk/cpk* homozygoytes and 26 phenotypically unaffected littermates. To confirm the phenotypic assignment in each cohort, each mouse was typed with the proximal chromosome 12 markers, *D12Mit218* and *D12Mit105*. As expected, the phenotypic mutants were all homozygous for B6 alleles of both markers and the phenotypically unaffected mice were either homozygous or heterozygous for CAST alleles of these markers.

Similarly, the 21 $F_2$ mutants from the (D2 × B6) intercross were homozygous for B6 alleles of both markers.

### Renal cystic disease as a quantitative trait

Different parameters were used to assess the severity of the renal cystic disease in each $F_2$ cohort because the phenotypic analyses were initiated at separate institutions. The concordance of the initial results suggested that these data could be reported together.

For the (B6 × CAST) intercross, previous analyses of $F_2$ *cpk/cpk* pups indicated that the ratio of kidney length to body length, using the distance from crown to rump (K/C–R), was a robust parameter to measure renal cystic disease severity as a quantitative trait. By correcting kidney length for body length, this ratio takes into account the potential growth retardation in suckling mutants. K/C–R was found to be distributed normally in the $F_2$ cohort and more variable than in B6-*cpk/cpk* mice (L.M. Guay-Woodford, unpublished data). In the (B6 × CAST) $F_2$ population generated for this study, K/C–R was again distributed normally.

For the (D2 × B6) intercross, both combined kidney weight and body weight were recorded for the $F_2$ *cpk/cpk* homozygotes. In order to correct kidney size for body size as described above, we used the ratio of combined kidney weight to body weight (KW/BW) as the quantitative trait and confirmed that KW/BW was distributed normally in this $F_2$ cohort.

Because the renal cystic disease severity was quantitated using different ratios in the two $F_2$ cohorts, we specifically examined the relationship between these parameters. Both K/C–R and KW/BW ratios were calculated for the (B6 × CAST) $F_2$ *cpk/cpk* pups ($n$ = 22) and phenotypically normal littermates ($n$ = 26). Linear regression analysis revealed that K/C–R and KW/BW are highly correlated in this single $F_2$ cohort ($r$ = 0.88).

### Biliary histopathology scored as a quantitative trait

We established the normal ranges for each feature in our semi-quantitative scoring system by analyzing the biliary histology in unaffected $F_2$ pups, i.e. those who were either homozygous or heterozygous for CAST alleles of the proximal chromosome 12 markers. In the analysis of $F_2$ *cpk/cpk* homozygotes, we scored each feature on a scale of 0–4, with 0 indicating the absence of pathology and 4 indicating severe pathological changes (maximum total score = 24). Although the features in the central and peripheral portal areas were well correlated, the histopathology associated with the central bile ducts/ductules was more readily apparent. Therefore, to calculate the biliary score, we summed the individual scores of the features in the central portal tracts. The mean biliary score in the unaffected $F_2$ pups was 4.2 [90% confidence interval (CI) 0–9.3], whereas the mean score in the $F_2$ *cpk/cpk* cohort was 18.6 (90% CI 15–22) and this parameter was distributed normally.

Representative sections of the central arborization from B6-*cpk/cpk* livers (no pathology), and livers from $F_2$ *cpk/cpk* pups with mild DPM (score = 13), moderate DPM (score = 18) and severe DPM (score = 23) are shown in Figure 1a–d. It is of note that those pups with the more severe DPM tended to have associated cystic abnormalities in both the pancreas and common bile duct (Fig. 1e). Given the limited size of this cohort, we were unable to assess the statistical significance of the latter.

Comparable biliary scores were obtained from analysis of the (D2 × B6) $F_2$ *cpk/cpk* cohort, although the number of bile ductules per portal vein was not assessed. The mean biliary score was 14.3 (90% CI 13–17) and the quantitative trait was distributed normally.

### Correlation between the renal cystic disease and biliary histopathology scored as quantitative traits

Our data indicate that, when measured as quantitative traits, the severities of both the renal cystic disease and the DPM vary in our $F_2$ cohorts. We hypothesize that this phenotypic variability is due to variation in the genetic background, in particular involving modifier loci whose alleles differ between B6 and either CAST or D2. As the first step towards determining whether the same QTLs modulate renal and biliary pathology in the *cpk* model, we examined the correlation between renal cystic disease and biliary histopathology using linear regression analysis. We found no correlation between K/C-R and the biliary score in the (B6 × CAST) $F_2$ *cpk/cpk* cohort ($r$ = 0.12) (Fig. 2a). Consistent with our evidence that K/C-R and KW/BW are highly correlated, no correlation was detected between KW/BW and the biliary score ($r$ = 0.36). Similarly, no correlation was found between KW/BW and the biliary score in the (D2 × B6) $F_2$ *cpk/cpk* cohort ($r$ = –0.05) (Fig. 2b).

### Analysis of heterozygotes derived from the D2 congenic strain

In the course of our analyses, we noted that aged +/*cpk* heterozygotes in the D2 congenic strain as well as (D2 × B6) $F_1$s developed abdominal distension. Gross pathological exam-

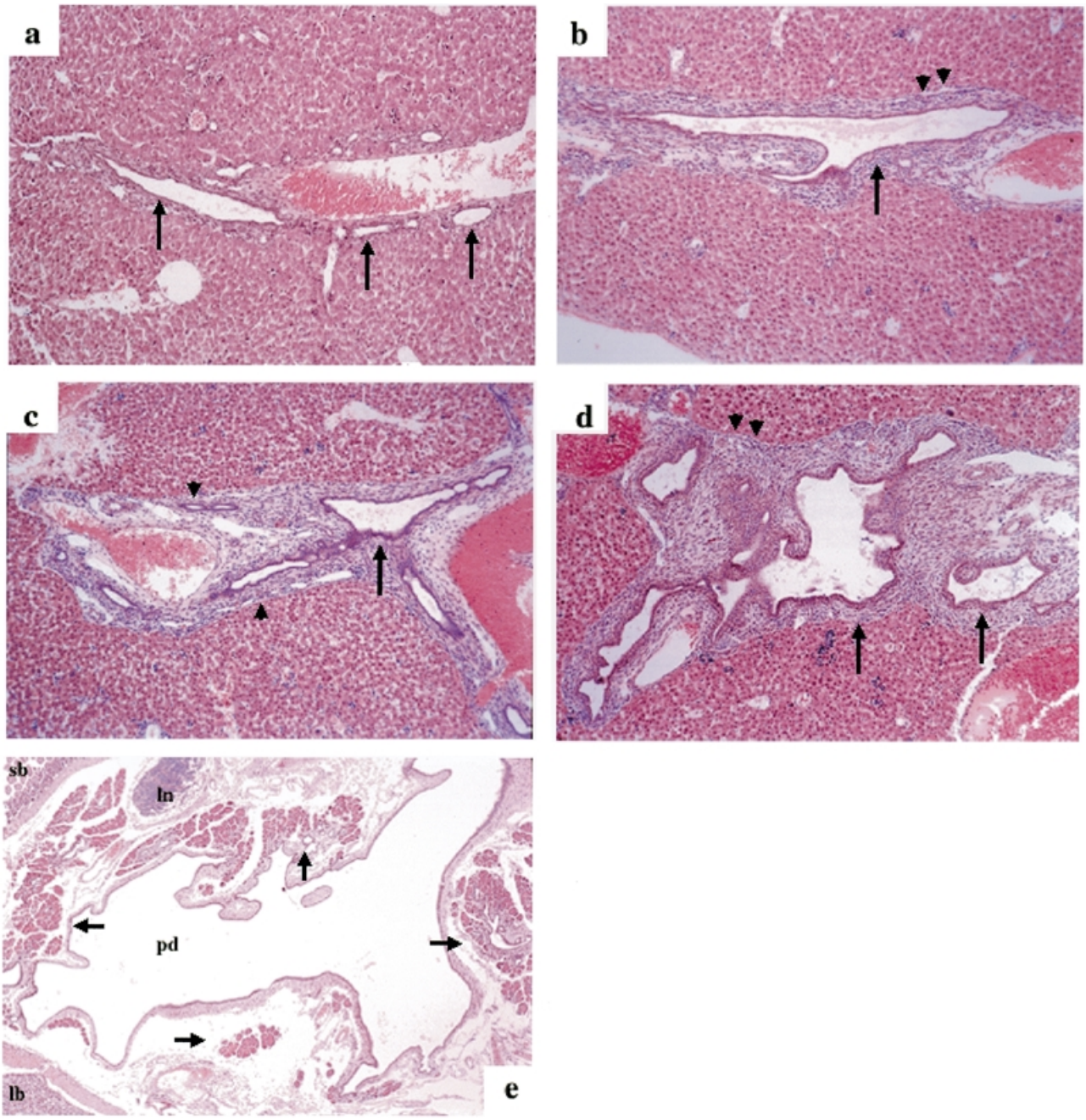


**Figure 1.** Representative central biliary histopathology. (a–d) Biliary histopathology in B6-*cpk*/*cpk* pups (**a**) and $F_2$ *cpk*/*cpk* pups from the (B6 × CAST) intercross with mild (**b**) DPM (score = 13), moderate (**c**) DPM (score = 18) and severe (**d**) DPM (score = 23). The arrows indicate the bile ducts and the arrowheads indicate peripherally placed bile ductules. Magnification, 100×. (**e**) Representative histopathological changes involving the pancreas in (B6 × CAST) $F_2$ *cpk*/*cpk* pups. The arrows indicate hypoplastic pancreatic tissue; sb, small bowel; ln, lymph node; lb, large bowel; pd, markedly dilated pancreatic duct. Magnification, 100×.

ination revealed cystic changes in the liver, with individual cysts ranging in size from 0.1 to 2.8 cm. A representative example is shown in Figure 3a.

More detailed analyses showed variability in both the number and character of the gross cysts. Thus, we scored each liver for the presence of cysts and categorized the cysts as simple or multilocular. Again, we employed a scale of 0–4, with 0 indicating no cysts and 4 indicating >10 cysts. The number of the liver cysts correlated with age in the D2 heterozygotes. In addition, there was suggestive evidence that females were affected more severely than males in both the D2 and $F_1$ cohorts, and pregnancy appeared to exacerbate the liver cystic disease. Histological examination indicated that both the simple and multilocular cysts probably arose from bile ducts/ductules. In addition, there was evidence for an associated DPM in both the D2 and $F_1$ cohorts. Although the biliary scores were variable in each cohort, the DPM was generally more severe in the $F_1$ +/*cpk* heterozygotes. These data are summarized in Table 1 and Figure 3b and c. It is of note that we found no evidence of associated renal cystic disease in any +/*cpk* heterozygotes.

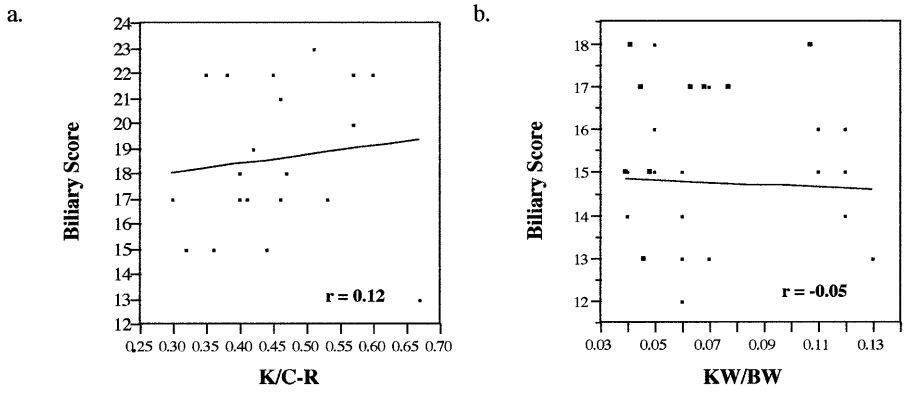


**Figure 2.** Correlation between the renal cystic disease and the DPM scored as quantitative traits. (**a**) The (B6 × CAST) $F_2$ *cpk/cpk* cohort. (**b**) The (D2 × B6) $F_2$ *cpk/cpk* cohort.

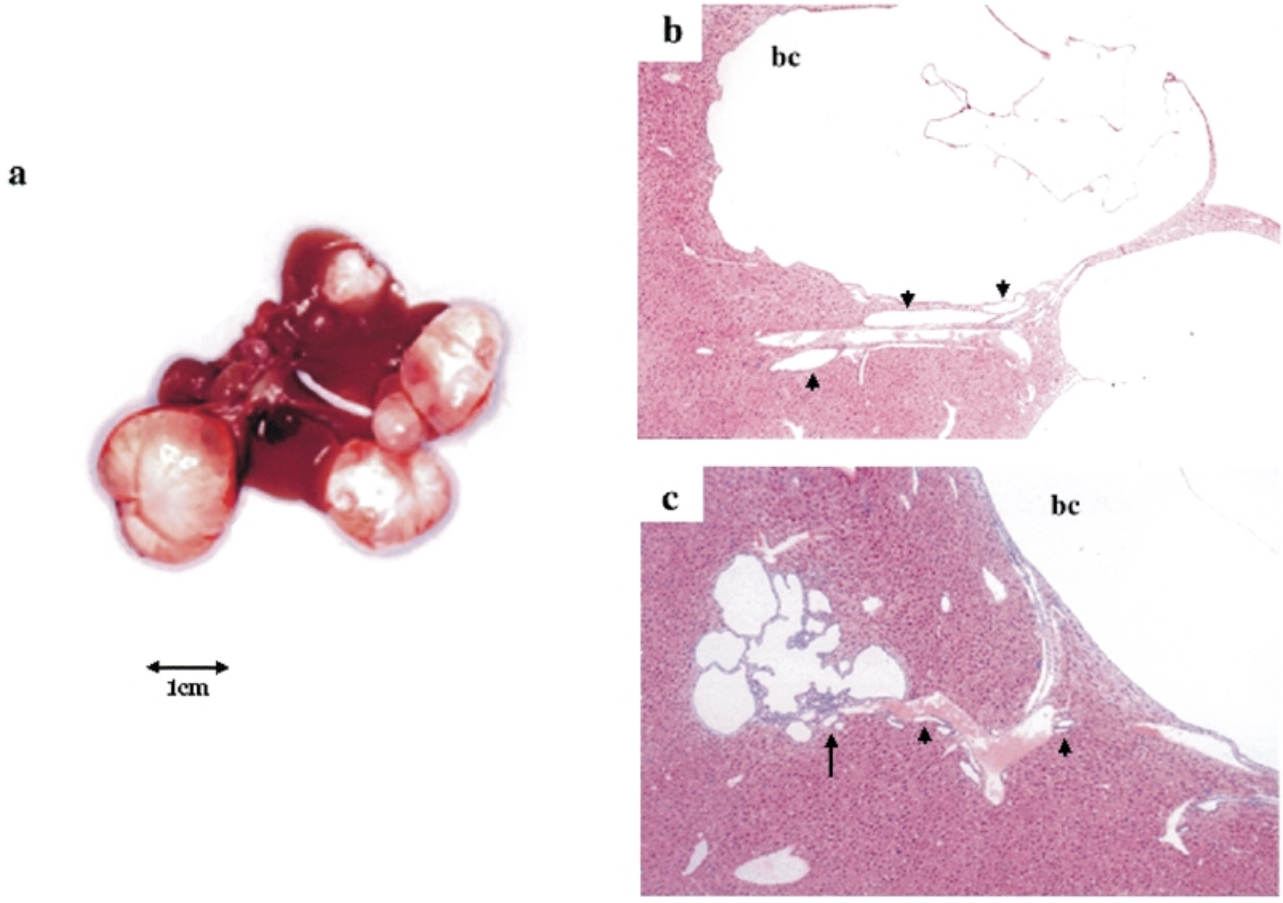


**Figure 3.** Biliary cysts in representative D2-+/*cpk* heterozygotes. (**a**) A representative example of liver cysts. Isolated cysts were observed in all lobes of the liver and ranged in size from 0.1 to 2.8 cm. Some cysts were simple in their architecture and some were multilocular. In the majority, the cystic fluid was clear. In a few, the fluid was either chylous or frankly hemorrhagic. (**b**) Representative biliary histopathology in D2-+/*cpk* heterozygotes. The proximity between the large cyst (bc) and adjacent bile ductules (arrowheads) suggests that the cyst was derived from biliary epithelium. Magnification, 40×. (**c**) Representative biliary histopathology in (D2 × B6) $F_1$ +/*cpk* heterozygotes. A large cyst lies adjacent to a portal tract. Bile ductules (arrowheads) apparently have undergone multilocular cystic transformation (arrow). Magnification, 40×.

### Chromosome 12 loss of heterozygosity in cyst cells

Our anatomical analyses indicated that biliary pathology occurs in +/*cpk* heterozygotes derived from the D2 congenic strain and develops in an age-dependent fashion. These observations are strikingly similar to those previously reported in both kidney and liver cysts from human ADPKD patients (29–31). We therefore hypothesized that the D2-+/*cpk* biliary changes could arise as the result of a similar mechanism, e.g. somatic loss of the wild-type *cpk* allele. To test this hypothesis, we analyzed the liver cysts for loss of heterozygosity (LOH).

In the D2 congenic mouse model, the B6-derived interval containing the *cpk* gene was introgressed into the D2 genetic background by serial backcrossing for six generations. Therefore, D2-+/*cpk* mice were heterozygous for proximal

**Table 1.** Semi-quantitative scoring of histopathology in D2.B6-+/*cpk* and (D2.B6-+/*cpk* × B6) $F_1$+/*cpk*

| | Age (months) | Gender | Simple cysts[a] | Multilocular cysts[b] | Biliary score[c] |
|---|---|---|---|---|---|
| D2.B6-+/*cpk* | | | | | |
| DB4.A | 4 | Female | 1 | 0 | 2 |
| DB4.B | 4 | Female | 1 | 1 | 4 |
| DB7.A | 7 | Male | 2 | 2 | 5 |
| DB7.B | 7 | Female | 0 | 0 | 4 |
| DB9.A | 9–10 | Female | 1 | 2 | 5 |
| DB9.B | 9–10 | Male | 2 | 0 | 7 |
| DB9.C | 9–10 | Male | 1 | 1 | 5 |
| DB9.D | 9–10 | Female | 3 | 3 | 7 |
| DB9.E | 9–10 | Female | 3 | 3 | 11 |
| DB9.F | 9–10 | Male | 1 | 1 | 7 |
| DB9.G | 9–10 | Male | 2 | 2 | 6 |
| DB9.H | 9–10 | Male | 1 | 1 | 9 |
| DB9.I | 9–10 | Female | 3 | 3 | 10 |
| DB9.J | 9 | Female | 4 | 4 | 18 |
| Mean | | | 1.9 ± 0.4 | 1.8 ± 0.4 | 8.5 ± 1.2 |
| (D2.B6-+/*cpk* × B6) $F_1$+/*cpk* | | | | | |
| F1.A | 10 | Female | 3 | 3 | 14 |
| F1.B | 10 | Female | 4 | 4 | 17 |
| F1.C | 10 | Female | 4 | 4 | 14 |
| F1.D | 10 | Male | 1 | 2 | 3 |
| F1.E | 10 | Female | 3 | 3 | 9 |
| F1.F | 10 | Female | 4 | 4 | 11 |
| F1.G | 10 | Female | 4 | 4 | 12 |
| F1.H | 10 | Female | 4 | 4 | 8 |
| F1.I | 10 | Female | 4 | 4 | 19 |
| Mean | | | 3.1 ± 0.4 | 3.2 ± 0.4 | 11.9 ± 1.6 |

Cysts were defined as either [a]simple, e.g. without lobulation or septae, or [b]multilocular, e.g. with lobulation and septae.

[c]Biliary score represents the sum of individual scores for the characteristics described in the text.

The mean scores for simple cysts, multilocular cysts and the biliary histpathology are provided as means ± SEM.

chromosome 12 markers and homozygous for D2 alleles at >96% of all other genomic markers. The B6-derived haplotype defined by the markers *D12Mit218* and *D12Mit105* contains the mutant *cpk* allele, whereas the D2-derived haplotype contains the wild-type *cpk* allele.

We prepared DNA from 17 liver cysts obtained from 11 D2-+/*cpk* animals and typed the markers *D12Mit218* and *D12Mit105* in both cyst-derived DNA and splenic DNA. PCR amplification was unsuccessful for one cyst. In 6 of the remaining 16 cysts (37.5%), we found evidence of LOH, i.e. the D2 allele for each marker was absent (Fig. 4). The cysts with evidence of LOH were obtained from six different animals. Four of these mice also had cysts with no evidence of LOH. These data are consistent with previous reports of LOH in renal and biliary cysts from human patients with ADPKD (29–31).

We then evaluated the extent of the LOH. Using the proximal chromosome 12 markers identified in Figure 5, we performed extended haplotype analysis in two animals from which we had obtained two cysts, one with and one without LOH. In those cysts with LOH, the loss of the D2 haplotype extended from *D12Mit182* to *D12Mit46*. A representative autoradiograph is shown in Figure 6.

In the D2 congenic construct, a discrete interval of B6-derived proximal chromosome 12 was introgressed into the D2 background. Therefore, our ability to detect the distal extent of the LOH region in D2-+/*cpk* biliary cysts was constrained by the size of the congenic interval, which did not extend beyond *D12Mit46*. Thus, the LOH region that we report represents the minimum size of the LOH interval. We note that further genetic analysis in $F_1$ heterozygotes from a (B6-+/*cpk* × wild-type D2) cross would allow us to distinguish between mitotic recombination and loss of the entire wild-type D2 chromosome as the mechanism underlying the LOH. These studies are in progress.

## DISCUSSION

In this study, we analyzed $F_2$ *cpk*/*cpk* homozygotes from two different intercrosses between B6 and either CAST or D2. We examined both the rapidly progressive renal cystic disease and the DPM as quantitative traits. Our data indicate that the

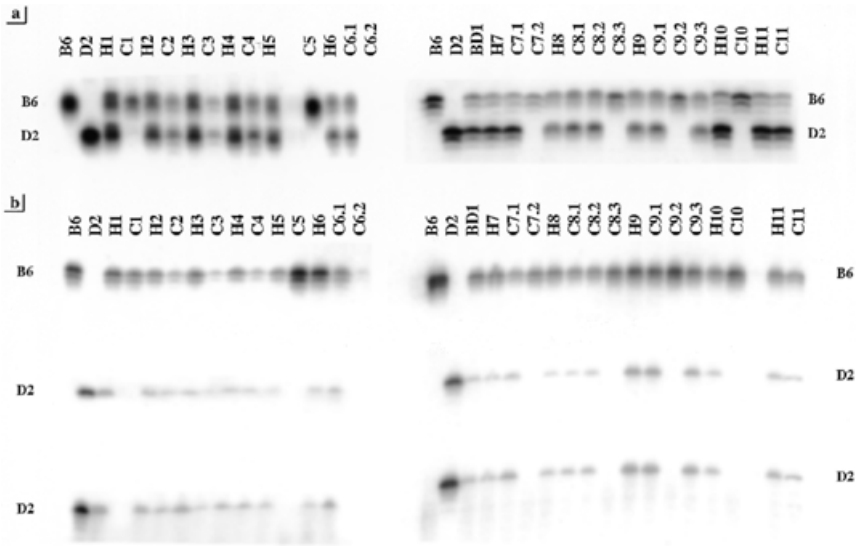


**Figure 4.** Loss of heterozygosity of *cpk*-linked polymorphic markers in cyst-derived epithelia from D2-+/*cpk* liver cysts. DNA from the B6 and D2 parental strains, a known heterozygote (BD1) and samples of genomic DNA (H1–H11) paired with cyst-derived DNA (C1–C11) from each D2-+/*cpk* heterozygote were analyzed with the chromosome 12 markers *D12Mit218* (**a**) and *D12Mit105* (**b**). Multiple cysts from the same animal are designated in sequential order, e.g. C6.1, C6.2. The B6 and D2 alleles of each marker are indicated. Amplification from one cyst (C6.2) failed. In epithelial-derived DNA from six cysts (C1, C5, C7.2, C8.3, C9.2 and C10), the D2 allele of each marker is absent, which is consistent with a somatic loss of the wild-type *cpk* allele.

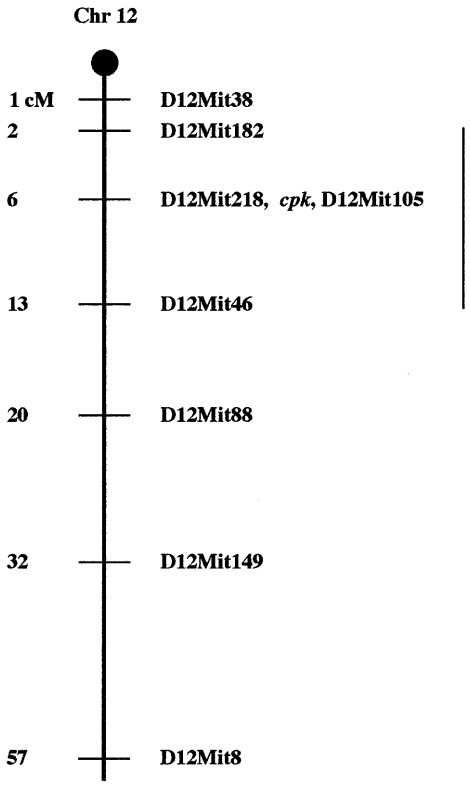


**Figure 5.** Genetic markers of chromosome 12. Markers and the relative position of the *cpk* locus are indicated on the right, and the distances for each marker from the centromere, as assigned by the MIT/Whitehead Center for Genome Research (http://www-genome.wi.mit.edu ), are indicated on the left. All distances are expressed in centimorgans (cM). The minimum extent of the LOH interval is indicated by the vertical bar.

phenotypic variability in each trait is modulated by genetic background, suggesting the presence of QTLs that modulate these phenotypes. We note, however, that the severity of the renal cystic disease, when measured as a quantitative trait, does not correlate with the severity of the DPM. This observation raises interesting mechanistic possibilities. For example, are there different sets of QTLs that modulate the progression of cystic disease phenotypes in the kidney and liver, irrespective of the primary genetic defect, or do *cpk*-specific QTLs exert organ-specific effects? Genetic mapping studies are in progress to identify these putative QTLs and to distinguish organ-specific versus disease-specific modifier effects.

The DPM is not expressed in B6-*cpk*/*cpk* homozygotes, but is evident in both of our $F_2$ cohorts. Since only one mutant allele has been described for the *cpk* model, we hypothesize that this variability reflects the presence of a QTL or set of QTLs that specifically modulate the biliary pathology. However, larger numbers of $F_2$ *cpk*/*cpk* mice will need to be characterized in order to determine whether the biliary phenotype is modulated by a limited number of B6 alleles or combinations of B6 and CAST or D2 alleles.

In this regard, it is interesting to note that the DPM evident in our (D2 × B6) $F_1$ +/*cpk* heterozygotes is more severe than that expressed in D2-+/*cpk* heterozygotes. The $F_1$ animals are heterozygous for B6 and D2 alleles at all loci, except for the *cpk* interval, whereas heterozygotes from the D2 congenic strain are homozygous for D2 alleles at all loci, except the *cpk* interval. Based on these data, we speculate that the presence of non-B6 alleles at the putative QTLs unmasks a biliary lesion in the *cpk* model and the disease severity is exacerbated by a possible epistatic interaction among B6 alleles and non-B6 alleles at these QTLs.

These observations have important implications for our plans to map the DPM-associated QTLs, as strategies for identifying epistatic interactions in conventional mapping crosses are less than ideal. In a standard whole-genome scan with dense marker coverage, the search for epistatic interactions would require testing of all pairwise combinations of markers. This approach is very computationally intensive (32). Moreover, with modest

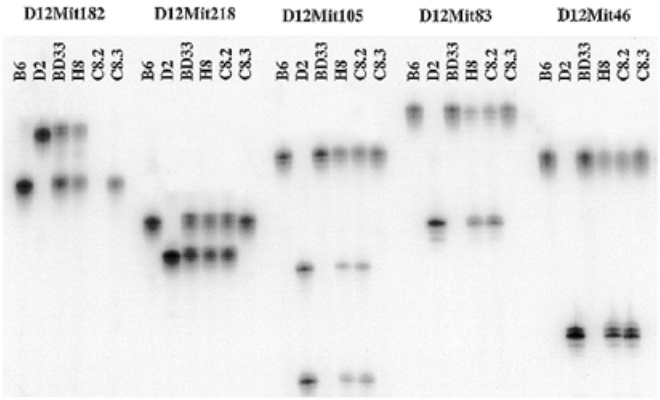


**Figure 6.** Extended haplotype analysis to define the LOH interval. Haplotype analysis using the proximal chromosome 12 markers reveals that the LOH interval in cyst C8.3 extends from *D12Mit182* to *D12Mit46*, a span of ~11 cM. The genotypes of the B6 and D2 parental strains, a key recombinant (BD33), from one of our *cpk* mapping crosses, and samples H8, C8.2 and C8.3 are shown.

sized data sets, e.g. <1000 progeny, it may be difficult to detect pairwise interactions between QTLs that surpass the genome-wide significance threshold. Upadhya *et al.* (24) have suggested that one approach to this problem is to evaluate those QTLs that have at least suggestive main effects in a pairwise fashion for epistatic interactions. The biological relevance of such putative QTLs and their epistatic interactions can then be examined further in specifically engineered congenic strains, as was done to evaluate modifier loci for the *jck* model of PKD (33).

In addition to examining the DPM as a quantitative trait, we also investigated the possible mechanisms underlying the development of biliary cysts in +/*cpk* heterozygotes. For these studies, we modified a previously described method (29). This technique minimizes contamination from other cell types, avoids the potential difficulties attendant with cultured cells and has proved to be a robust method for evaluating LOH in renal and biliary cysts. Among the 16 cysts evaluated using tightly linked markers, we detected LOH for the *cpk* interval in six cysts (38%). Given that the *cpk* gene has yet to be cloned, we were unable to refine these analyses further in the remaining 10 cysts (62%) by including a search for possible intragenic mutations. However, we note that recent examination of biliary cysts from a cohort of human ADPKD patients revealed LOH of intragenic markers as well as specific intragenic point mutations involving the *PKD1* gene (31). Moreover, in the *Pkd2* mouse model, somatic inactivation of the unstable WS25 allele resulted in biliary cysts in 100% of $Pkd2^{WS25/-}$ mutants (34). We therefore speculate that somatic loss of the wild-type allele at the *cpk* locus, through either chromosomal loss or specific intragenic mutations, may also be the rate-limiting step in the formation of focal biliary cysts in +/*cpk* heterozygotes.

It is interesting to note that focal biliary cysts have been observed in B6-+/*cpk* heterozygotes (35), as well as in $F_1$ +/*cpk* heterozygotes derived from crosses with CD-1 (26), BALB/c (27) and D2 (this study). We therefore speculate that the putative loss of the wild-type *cpk* allele is due to factors intrinsic to either the *cpk* gene or the *cpk* interval on chromosome 12, rather than the consequence of epigenetic modulation. On the contrary, renal cysts were not detected in +/*cpk* heterozygotes either in this study or in previous reports. Therefore, for reasons that currently are inexplicable, it appears that the local milieu in the biliary tract, but not in the kidney, is conducive for LOH-associated pathology. This is somewhat surprising given that renal cystic disease is invariably found in *cpk*/*cpk* homozygotes whereas expression of the biliary phenotype is more variable. Further investigations of these phenomena must await the identification and characterization of the *cpk* gene.

Finally, we propose that expression of the DPM in *cpk*/*cpk* homozygotes and the development of biliary cysts in the +/*cpk* heterozygotes may be developmentally related manifestations of the same underlying mechanism. During liver organogenesis, biliary development initiates from a layer of hepatic precursor cells that coalesce to form a sleeve-like layer around the portal vein and its ramifications. This sleeve, representing the first anlage of the intrahepatic bile ducts, then duplicates to form a double-layered sleeve of cytokeratin-rich cells, referred to as the ductal plate (DP) (reviewed in ref. 36). As a result of reciprocal interactions between the ductal plate epithelia and the mesenchyme surrounding the portal vein branches, short segments of the DP give rise to bile ductules (37–39). These ductules are then incorporated into the periportal mesenchyme and the non-tubular elements of the ductal plate are absorbed. Thus, during successive periods of liver development, DP remodeling leads to the formation of the intrahepatic biliary tree. The largest ducts are formed first, followed by segmental, interlobular and finally by the smallest bile ductules. Arrest or derangements in remodeling lead to the persistence of primitive bile duct configurations, or to what Jorgensen termed the DPM (40). The occurrence of DPM at different generations of the developing biliary tree gives rise to different clinico-pathological entities, e.g. Caroli's syndrome, congenital hepatic fibrosis and biliary cysts (41).

In our *cpk* crosses, the DPM is expressed very early in $F_2$ *cpk*/*cpk* homozygotes and biliary cysts are not observed. Therefore, the DPM may predominate when there is a germline loss of function of the *cpk* gene and the entire sequence of biliary development is affected. In comparison, biliary cysts are the predominant finding in aged +/*cpk* heterozygotes and can occur without associated biliary histopathology (Table 1). In this regard, we note that there is a subtle difference in the biliary abnormality expressed in aged heterozygotes versus young homozygous mutants, namely the DPM in +/*cpk* heterozygotes is dominated more by ductular branching and biliary epithelial hyperplasia than the presence of immature stroma and mesenchymal cells. Therefore, although somatic loss of the wild-type *cpk* allele also appears to perturb biliary differentiation, this effect seems to involve the epithelia more than the associated mesenchyme, resulting in focal proliferation and cyst formation.

In summary, we have characterized the renal and biliary phenotypes in both $F_2$ *cpk*/*cpk* homozygotes and +/*cpk* heterozygotes from two experimental crosses. The *cpk* allele appears to contain an inactivating mutation which disrupts tubulo-epithelial differentiation in the renal collecting ducts and the biliary tract. The pathogenesis of the renal cystic disease and early-onset DPM requires germline loss of function of the *cpk* gene. Although genetic modifiers apparently modulate the expression of both traits, different QTL effects appear to be operative in the kidney and the biliary tract. In addition, DPM and biliary cyst formation occur in aged heterozygotes through an apparent somatic loss of the wild-type *cpk* allele, and these

phenotypes appear to be modulated by genetic modifiers. QTL mapping studies will be required to determine the relationship among the modifiers that affect the different biliary phenotypes. The elucidation of these genes and their molecular interactions should provide novel insights into the complex pathogenesis of biliary ductal abnormalities in the *cpk* mouse and, given the phenotypic parallels, should shed light on the pathogenesis of the biliary abnormalities in human PKD as well.

## MATERIALS AND METHODS

### Mice

For the current study, two sets of experimental crosses were designed. First, C57BL/6J-+/*cpk* mice (B6-+/*cpk*), from a stock colony maintained at the University of Alabama at Birmingham, were bred to CAST mice purchased from the Jackson Laboratory (Bar Harbor, ME). $F_1$ progeny heterozygous for the *cpk* mutation were identified by test crossing and intercrossed. Initially, offspring affected with cystic kidney disease died between 8 and 15 days after birth. Therefore, subsequent $F_2$ litters were sacrificed 10 days after birth. Those $F_2$ pups sacrificed at earlier or later time points were excluded from these analyses.

For the second cross, a D2-+/*cpk* congenic line was generated. B6-+/*cpk* mice, from a stock colony maintained at the Brigham and Women's Hospital, were crossed to DBA/2J (D2) mice purchased from the Jackson Laboratory. Proven heterozygotes were backcrossed serially to the D2 strain for six generations, at which time >96% of the genome was D2-derived. D2-+/*cpk* heterozygotes were then crossed to wild-type B6 mice and proven $F_1$ heterozygotes were intercrossed. Only those $F_2$ *cpk*/*cpk* homozygotes sacrificed at 10 days of age were included in these analyses.

### Characterization of the renal cystic disease as a quantitative trait in $F_2$ mutants

To score the severity of the renal cystic disease as a quantitative trait, we measured either the K/C–R in $F_2$ homozygotes from the (B6-+/*cpk* × CAST) $F_1$ intercross or the KW/BW in $F_2$ homozygotes from the (D2-+/*cpk* × B6) $F_1$ intercross.

### Evaluation of the biliary ductal histopathology

For analyses of the $F_2$ cohort, livers were harvested from 10-day-old pups, fixed in alcoholic formalin (10% formalin in 70% ethanol) and embedded in paraffin to yield either a longitudinal or transverse section of the biliary arborization within each lobe. Sections were prepared at 5 μm thickness and stained with hematoxylin and eosin for light microscopy.

The mouse liver is composed of four lobes (from anterior to posterior): (i) a large median lobe partially divided into left and right parts by a ventral bifurcation containing the gall bladder; (ii) a large left lateral lobe; (iii) a small right lateral lobe having anterior and posterior divisions; and (iv) a still smaller caudal lobe consisting of two small, leaf-shaped parts (42). To standardize the analysis of central versus peripheral bile ducts/ductules, we modified the method described previously by Nauta *et al*. (7).

The median, right lateral and caudal lobes were embedded so that their convex or flat surfaces were parallel to the block surface and, thus, their arborizing biliary trees were sectioned primarily in the longitudinal plane. The left lobe was sectioned transversely at right angles to its flat surface and at ~5 μm intervals across the entire lobe to give longitudinal views of the bile ducts/ductules emanating from the hilus. Bile ducts/ductules and portal triads were examined systematically in each section by two blinded observers (J.R.L. and L.M.G.-W.).

For histopathological analyses of the D2-+/*cpk* heterozygotes and (D2-+/*cpk* × B6) $F_1$ heterozygotes, livers were harvested from animals at specified ages and prepared in a similar fashion.

### Characterization of the biliary ductal pathology as a quantitative trait

The DPM associated with human ARPKD is characterized by three key features: (i) 'chaotic' branching and dilatation of the bile ductules; (ii) biliary epithelial hyperplasia; and (iii) immature stroma within the portal triad (2).

We designed a semi-quantitative, histopathological scoring system to incorporate each of these features in the assessment of the portal triad. In each liver section, the central and peripheral portal areas were assessed for the following: (i) number of bile ducts/ductules per portal vein (an index of ductule branching); (ii) degree of bile duct/ductule branching in a single plane of section; (iii) extent of bile duct/ductule dilatation; (iv) degree of biliary duct epithelial hyperplasia; (v) amount of immature stroma in the portal triads; and (vi) degree of stromal cellularity in the portal tracts. For the (B6 × CAST) $F_2$ cohort, livers from *cpk*/*cpk* homozygotes, as well as age-matched, phenotypically normal pups were scored for all six characteristics. In the (D2 × B6) $F_2$ *cpk*/*cpk* homozygotes as well as the D2-+/*cpk* and $F_1$ +/*cpk* heterozygotes, all characteristics were scored, except the number of ductules per portal vein.

We also scored the gross livers and histological sections from the D2-+/*cpk* and $F_1$ +/*cpk* heterozygotes for the extent and nature (simple versus multilocular) of cystic changes.

### Preparation of epithelial cells from liver cysts

D2-+/*cpk* animals ($n$ = 11) were euthanized with ketamine. The cystic livers were excised and maintained at 4°C. Cystic epithelia were prepared using a modification of the method originally described by Qian *et al*. (29). Briefly, the surface of each cyst was rinsed with phosphate-buffered saline (PBS). The fluid content was drained by needle aspiration and the needle was left in place for the duration of the experiment. The cavity of each cyst was lavaged a minimum of three times with $Ca^{2+}$- and $Mg^{2+}$-free phosphate-buffered saline (PBS). PBS containing 2 mM EDTA was then injected into the cyst. Those cysts that maintained their volume following a 10–15 min incubation were considered intact. The extraction solution (PBS–EDTA) was drained by aspiration and centrifuged at 14 000 *g* (Eppendorf microcentrifuge) for 10 s. DNA was prepared from the pellet using the Puregene DNA extraction kit (Gentra Systems, Minneapolis, MN) according to the manufacturer's protocol. Ten micrograms of glycogen were added to each sample to assist in DNA precipitation.

### Genetic analysis

DNA for microsatellite analysis was prepared from liver cyst epithelia as above and from the spleens of each animal as

previously described (28). We previously have mapped the *cpk* locus to a proximal chromosome 12 interval tightly linked to the markers *D12Mit218* and *D12Mit105* (Fig. 5) (28,43). PCR amplification of each liver cyst- and spleen-derived DNA was performed using microsatellite markers from proximal chromosome 12 (*D12Mit38*, *D12Mit182*, *D12Mit218*, *D12Mit105* and *D12Mit46)* (44). PCR primer pairs were purchased from Research Genetics (Huntsville, AL).

Forward primers were end-labeled with [$\gamma$-$^{32}$P]ATP, and PCR amplification was performed as previously described (28). Amplified fragments were separated on denaturing 6% polyacrylamide gels and analyzed by autoradiography. All experiments were performed in triplicate. LOH was defined as loss of the D2 allele in liver cyst-derived DNA.

## ACKNOWLEDGEMENTS

The authors thank Feng Qian (Johns Hopkins University School of Medicine) for helpful discussions. William Collier and Christopher Wright provided technical assistance. This work was supported by National Institutes of Health grants DK51034 (L.M.G.-W.) and DK45639 (D.R.B.). The University of Alabama at Birmingham and the Brigham and Women's Hospital are fully accredited by the Association for the Assessment and Accreditation of Laboratory Animal Care.

## REFERENCES

1. Gabow, P. and Grantham, J. (1997) Polycystic kidney disease. In Schrier, R. and Gottschalk, C. (eds), *Diseases of the Kidney*. Little, Brown, Boston, MA, pp. 521–560.
2. Guay-Woodford, L. (1996) Autosomal recessive disease: clinical and genetic profiles. In Watson, M. and Torres, V. (eds), *Polycystic Kidney Disease*. Oxford University Press, Oxford, pp. 237–267.
3. Schieren, G., Pey, R., Bach, J., Hafner, M. and Gretz, N. (1996) Murine models of polycystic kidney disease. *Nephrol. Dial. Transplant.*, **11**, 38–45.
4. Preminger, G., Koch, W., Fried, F., McFarland, E., Murphy, E. and Mandell, J. (1982) Murine congenital polycystic kidney disease: a model for studying development of cystic disease. *J. Urol.*, **127**, 556–560.
5. Fry, J., Koch, W., Jennette, J., McFarland, E., Fried, F. and Mandell, J. (1985) A genetically determined murine model of infantile polycystic kidney disease. *J. Urol.*, **134**, 828–833.
6. Takahashi, H., Calvet, J., Dittemore-Hoover, D., Yoshida, K., Grantham, J. and Gattone, V. (1991) A hereditary model of slowly progressive polycystic kidney disease in the mouse. *J. Am. Soc. Nephrol.*, **1**, 980–989.
7. Nauta, J., Ozawa, Y., Sweeney, W., Rutledge, J. and Avner, E. (1993) Renal and biliary abnormalities in a new murine model of autosomal recessive polycystic kidney disease. *Pediatr. Nephrol.*, **7**, 163–172.
8. Atala, A., Freeman, M., Mandell, J. and Beier, D. (1993) Juvenile cystic kidneys (*jck*): a new mutation in the mouse which predisposes to the development of polycystic kidneys. *Kidney Int.*, **43**, 1081–1085.
9. Janaswami, P., Birkenmeier, E., Cook, S., Rowe, L., Bronson, R. and Davisson, M. (1997) Identification and genetic mapping of a new polycystic kidney disease on mouse chromosome 8. *Genomics*, **40**, 101–107.
10. Flaherty, L., Bryda, E., Collins, D., Rudofsky, U. and Montgomery, J. (1995) New mouse model for polycystic kidney disease with both recessive and dominant gene effects. *Kidney Int.*, **47**, 552–558.
11. Moyer, J., Lee-Tischler, M., Kwon, H.-Y., Schrick, J., Avner, E., Sweeney, W., Godfrey, V., Cacheiro, N., Wilkinson, J. and Woychik, R. (1994) Candidate gene associated with a mutation causing recessive polycystic kidney disease in mice. *Science*, **264**, 1329–1333.
12. Trudel, M., D'Agati, V. and Costantini, F. (1991) C-myc as an inducer of polycystic kidney disease in transgenic mice. *Kidney Int.*, **39**, 665–671.
13. Kelley, K., Agarwal, N., Reeders, S. and Herrup, K. (1991) Renal cyst formation and multifocal neoplasia in transgenic mice carrying the simian virus 40 early region. *J. Am. Soc. Nephrol.*, **2**, 84–97.
14. Keller, S., Jones, J., Boyle, A., Barrow, L., Killen, P., Green, D., Kapousta, N., Hitchcock, P., Swank, R. and Meisler, M. (1994) Kidney and retinal defects (*Krd*), a transgene-induced mutation with a deletion of mouse chromosome 19 that includes the *Pax2* locus. *Genomics*, **23**, 309–320.
15. Veis, D., Sorenson, C., Shutter, J. and Korsmeyer, S. (1993) Bcl-2-deficient mice demonstrate fulminant lymphoid apoptosis, polycystic kidneys, and hypopigmented hair. *Cell*, **75**, 229–240.
16. MacKay, K., Striker, L., Pinkert, C., Brinster, R. and Striker, G. (1987) Glomerulosclerosis and renal cysts in mice transgenic for the early region of SV40. *Kidney Int.*, **32**, 827–837.
17. Schaffner, D., Barrios, R., Massey, C., Banez, E., Ou, C., Rajagopalan, S., Aguilar-Cordova, E., Lebovitz, R., Overbeek, P. and Lieberman, M. (1993) Targeting of the rasT24 oncogene to the proximal convoluted tubules in transgenic mice results in hyperplasia and polycystic kidneys. *Am. J. Pathol.*, **142**, 1051–1060.
18. Lowden, D., Lindemann, G., Merlino, G., Barash, B., Calvet, J. and Gattone, V. (1994) Renal cysts in transgenic mice expressing transforming growth factor-$\alpha$. *J. Lab. Clin. Med.*, **124**, 386–394.
19. Lander, E. and Botstein, D. (1989) Mapping Mendelian factors underlying quantitative traits using RFLP linkage maps. *Genetics*, **121**, 185–199.
20. Iakoubova, O., Dushkin, H., Pacella, L. and Beier, D. (1999) Genetic analysis of modifying loci on mouse chromosome 1 affecting severity in a model of recessive polycystic kidney disease. *Physiol. Genomics*, **1**, 101–105.
21. Iakoubova, O., Dushkin, H. and Beier, D. (1995) Localization of a murine recessive polycystic kidney disease mutation and modifying loci that affect disease severity. *Genomics*, **26**, 107–114.
22. Woo, D., Miao, S. and Tran, T. (1995) Progression of polycystic kidney disease in *cpk* mice is a quantitative trait under polygenic control. *J. Am. Soc. Nephrol.*, **6**, 731A.
23. Woo, D., Nguyen, D., Khatibi, N. and Olsen, P. (1997) Genetic identification of two major modifier loci of polycystic kidney disease progression in *pcy* mice. *J. Clin. Invest.*, **100**, 1934–1940.
24. Upadhya, P., Churchill, G., Birkenmeier, E., Barker, J. and Frankel, W. (1999) Genetic modifiers of polycystic kidney disease in intersubspecific KAT2J mutants. *Genomics*, **58**, 129–137.
25. Guay-Woodford, L., Wright, C., Walz, G. and Churchill, G. (2000) Quantitative trait loci (QTLs) that influence renal cystic disease severity in the mouse *bpk* model. *J. Am. Soc. Nephrol.*, in press.
26. Gattone, V., MacNaughton, K. and Kraybill, A. (1996) Murine autosomal recessive polycystic kidney disease with multiorgan involvement induced by the *cpk* gene. *Anat. Rec.*, **245**, 488–499.
27. Ricker, J., Rankin, C., Calvet, J. and Gattone, V. (1999) Autosomal recessive polycystic kidney disease in BALB/c-*cpk/cpk* mice. *J. Am. Soc. Nephrol.*, **10**, A2142.
28. Simon, E., Cook, S., Davisson, M., D'Eustachio, P. and Guay-Woodford, L. (1994) The mouse congenital polycystic kidney (*cpk*) locus maps within 1.3 cM of the chromosome 12 marker *D12Nyu2*. *Genomics*, **21**, 415–418.
29. Qian, F., Watnick, T., Onuchic, L. and Germino, G. (1996) The molecular basis of focal cyst formation in human autosomal dominant polycystic kidney disease type I. *Cell*, **87**, 979–987.
30. Brasier, J. and Henske, E. (1997) Loss of the polycystic kidney disease (PKD1) region of chromosome 16p13 in renal cyst cells supports a loss-of-function model for cyst pathogenesis. *J. Clin. Invest.*, **99**, 194–199.
31. Watnick, T., Torres, V., Gandolph, M., Qian, F., Onuchic, L., Klinger, K., Landes, G. and Germino, G. (1998) Somatic mutation in individual liver cysts supports a two-hit model of cystogenesis in autosomal dominant polycystic kidney disease. *Mol. Cell*, **2**, 247–251.
32. Manly, K. and Olson, J. (1999) Overview of QTL mapping software and introduction to map manager QT. *Mamm. Genome*, **10**, 327–334.
33. Kuida, S. and Beier, D. (2000) Genetic localization of interacting modifiers affecting severity in a murine model of polycystic kidney disease. *Genome Res.*, **10**, 49–54.
34. Wu, G., D'Agati, V., Cai, Y., Markowitz, G., Park, J., Reynolds, D., Maeda, Y., Le, T., Hou, H., Kucherlapati, R. *et al*. (1998) Somatic inactivation of *Pkd2* results in polycystic kidney disease. *Cell*, **93**, 177–188.
35. Crocker, J., Belcher, S., Givner, M. and McCarthy, S. (1987) Polycystic kidney and liver disease and corticosterone changes in the cpk mouse. *Kidney Int.*, **31**, 1088–1091.
36. Desmet, V. (1998) Pathogenesis of ductal plate abnormalities. *Mayo Clin. Proc.*, **73**, 80–89.
37. Van Eychen, P., Sciot, R. and Callea, F. (1988) The development of the intrahepatic bile duct in man: a keratin-immunohistochemical study. *Hepatology*, **8**, 1586–1595.
38. Van Eycken, P., Sciot, R. and Desmet, V. (1988) Intrahepatic bile duct development in the rat: a cytokeratin-immunohistochemical study. *Lab. Invest.*, **59**, 52–59.

39. Shah, K. and Gerber, M. (1990) Development of intrahepatic bile ducts in humans; immunohistochemical study using monoclonal cytokeratin antibodies. *Arch. Pathol.*, **114**, 597–600.
40. Jorgensen, M. (1977) The ductal plate malformation: a study of the intrahepatic bile-duct lesion in infantile polycystic disease and congenital hepatic fibrosis. *Acta Pathol. Microbiol. Scand.*, **257**(suppl.), 1–88.
41. D'Agata, I., Jonas, M., Perez-Atayde, A. and Guay-Woodford, L. (1994) Combined cystic disease of the liver and kidney. *Semin. Liver Dis.*, **14**, 215–228.
42. Maronpot, R. (1999) Normal liver and gallbladder. In Maronpot, R. (ed.), *Pathology of the Mouse*. Cache River Press, Vienna, IL, pp. 120–124.
43. DasGupta, S., Stockwin, J. and Guay-Woodford, L. (1996) Physical mapping of the interval containing the mouse *cpk* mutation. *J. Am. Soc. Nephrol.*, **7**, A1725.
44. Loh, N., Ambrose, H., Guay-Woodford, L., DasGupta, S., Nawrotzki, R., Blake, D. and Davies, K. (1998) Genomic organization and refined mapping of the mouse β-dystrobrevin gene. *Mamm. Genome*, **9**, 857–862.